Impact of structural imperfections on the energy-level alignment in organic films

T. Hosokai,[1,*] H. Machida,[2] A. Gerlach,[1] S. Kera,[2] F. Schreiber,[1] and N. Ueno[2,†]

[1]*Institut für Angewandte Physik, Universität Tübingen, Auf der Morgenstelle 10, Tübingen D-72076, Germany*

[2]*Department of Nanomaterial Science, Graduate School of Advanced Integration Science, Chiba University, 1-33 Yayoi-cho, Inage-ku, Chiba 263-8522, Japan*

(Received 24 January 2011; revised manuscript received 18 March 2011; published 9 May 2011)

This paper reports that structural imperfection in an organic thin film modulates the electronic structure to result in a serious band bending and change in the energy-level alignment (ELA) at the organic-conductor interface. Ultraviolet photoelectron spectroscopy (UPS) and metastable atom electron spectroscopy (MAES) were adopted to investigate thickness dependences of the electronic structure of polar phthalocyanine (chlorogallium phthalocyanine) thin films grown on graphite with respect to the film structure. We observed a large band-bending–like shift of occupied molecular-orbital bands toward the Fermi level and a continuous increase in the vacuum level for the as-grown film, whereas these phenomena were considerably suppressed by annealing the film. Both the as-grown and annealed films were characterized as essentially the same stacked bilayer film structure; however, high-resolution UPS and MAES measurements evidenced that there are structural defects in the as-grown film but not clearly in the annealed film, indicating that the defects are the origin of the modulation of the ELA and the band bending. Controlling the structural imperfections is a key issue for the desired ELA in organic devices.

DOI: 10.1103/PhysRevB.83.195310 PACS number(s): 73.20.−r, 79.60.−i, 68.35.bm, 81.05.Fb

I. INTRODUCTION

During past decades, great effort has been dedicated to thorough investigations of the energy-level alignment (ELA) at organic-conductor and organic-organic interfaces and the band bending in organic thin films to unravel origins of these phenomena.[1–17] It was reported that there are band-bending phenomona in organic thin films, which do not necessarily originate from the well-known mechanism in inorganic semiconductors but from changes in molecular orientation in the films.[16,18–21] As all band-bending phenomena observed at thermal equilibrium condition of the relevant electron system are related to the Fermi level position in the organic band gap, we consider the band-bending phenomena to be within the category of ELA effects. Accordingly, an important open issue, which still remains elusive, is the influence of the structure of organic films on the ELA. Such influence appears drastically in the electronic structure of various organic films and especially of films of *polar* molecules, because intramolecular local electric dipoles in a nonpolar molecule as well as permanent electric dipole (P) of a polar molecule affect critically the ELA depending on the molecular packing or orientation.[16,18–22] It is expected that these phenomena impact seriously on charge-transport properties of organic devices. For example, Kaji *et al.* demonstrated recently for chloroaluminum phthalocyanine (ClAlPc) thin-films-based organic field-effect transistors (OFETs) that the Fermi level could be controlled widely in between the highest occupied molecular orbital (HOMO) and the lowest unoccupied MO of the films by applying an annealing procedure, and succeeded in tuning the type of charge carrier and the device performance.[23]

Among several successful uses of polar molecules for organic devices,[23–29] the correlation between their film structures and the ELA is not yet well explored and thus still remains vague. For ultrathin films of various polar metal-Pc (p-MPc) molecules deposited on a molybdenum disulfide (MoS_2) (ClAlPc[30–33]) and a highly oriented pyrolytic graphite (HOPG) (OTiPc,[34–37] OVPc,[38] ClAlPc,[39,40] and PbPc[41]), we have thoroughly studied their film structure and growth, and evolution of electronic structure in these films using mainly ultraviolet photoelectron spectroscopy (UPS), metastable atom electron spectroscopy (MAES), and other electron spectroscopic methods. It was observed that, for the films grown at room temperature, a series of the p-MPc molecules form stacked bilayer islands or domains from (sub)monolayer thickness, where molecules arrange in a cofacial configuration to cancel their own P as schematically shown in Fig. 1(b) (left panel). However, the bilayer domains in the monolayer films were found to be in a metastable structure with imperfect stacking, and this structure was driven to a stable monolayer in which all the molecules are oriented flat with the oxygen (for OTiPc and OVPc) or chlorine atom (for ClAlPc) directed outward to the vacuum by an annealing procedure.[33–40,42] Moreover, a combination study of microspot UPS and photoemission electron microscopy on a PbPc/HOPG system indicated that both the as-grown (AG) and annealed (AN) bilayer islands or domains have essentially the same stacked structure but with different molecular packing and domain sizes; the AG (AN) film can be regarded as short-range-ordered loosely packed (long-range-ordered closely packed) film.[43]

In this paper, we aim to clarify how such a structural difference in ultrathin films of p-MPc influences the thicker film structure on HOPG and the resulting ELA as well as band-bending phenomena. Chlorogallium Pc [ClGaPc, Fig. 1(a)] employed here is a representative of shuttlecock-type p-MPc similar to ClAlPc and has a large P of 3.78 Debye.[44–47] The extremely inert surface of HOPG, which can avoid a strong electronic interaction with organic overlayer molecules (the work function shifts by only $\sim$0.05 eV), enables us to relate the electronic structure of the organic thin films directly to the film structure.[5,10,22,35,41] We compared the thickness (δ) dependences of the electronic structure of the AG and AN films of ClGaPc and found that a very large band bending

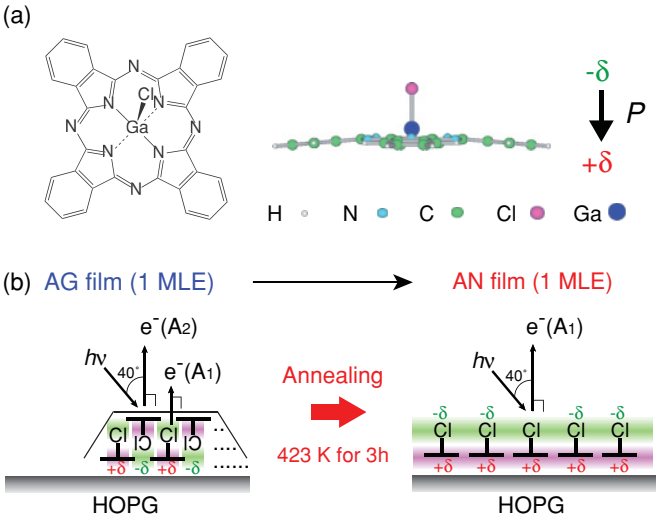

FIG. 1. (Color online) (a) Chemical structure and molecular conformation of ClGaPc and the direction of the dipole moment P. (b) Schematic of the structural rearrangement of a stacked bilayer domain into a well-ordered monolayer film (dipole layer). The assignment of different electron emissions from the first (A_1) and second (A_2) layers in the UPS measurements is shown.

appears in the AG film and is considerably suppressed by annealing the film. A combination of high-resolution UPS and MAES measurements rationalized the large band bending by the structural defects in the AG films, which originate from imperfections of the molecular packing structure. Our results demonstrate that control of the structural imperfection is a prerequisite for a desired ELA of p-MPc thin films beyond the ultrathin regime.

II. EXPERIMENT

He I UPS and MAES experiments were carried out at Chiba University using a home-built UHV system equipped with a PHOIBOS-HSA100 analyzer (energy resolution was set to be 60 meV).[48] UPS spectra were measured at a light incident angle of 40° and electron emission angles of 0° (normal emission), while MAES spectra were at incident and emission angles of 45°. A HOPG (ZYA-grade) substrate was cleaved in air just before being loaded into the preparation chamber ($\sim 6 \times 10^{-8}$ Pa) and cleaned by *in situ* heating at 673 K for 24 h. ClGaPc purchased from Sigma-Aldrich Co. (purity > 97%) was purified by vacuum sublimation and was thoroughly outgassed in the preparation chamber before use. The AG and AN films were prepared on the clean HOPG substrates kept at 295 K (deposition rate: 0.03–0.05 nm/min measured with a quartz microbalance). For the measurements of the AN films, we repeatedly conducted the deposition, sample annealing at 425 K for 3 h, and UPS/MAES measurements at 295 K, whereas the measurements of the AG films were performed similarly without annealing. The annealing condition was determined according to the well-established procedure for preparation of a highly and long-range-ordered p-MPc monolayer film with negligible molecular desorption during the annealing.[10] In this paper, the nominal thickness (δ) of the films is expressed by a monolayer equivalent coverage (MLE) that is defined as the molecular amount where the closely packed molecules with their molecular plane oriented parallel to the substrate form a monolayer. The 1 MLE (= 0.35 nm) was determined by saturation of the vacuum level (VL) shift due to completion of the dipole layer formation originating from the well-ordered monolayer of the AN film[35,41] and by disappearance of substrate features in MAES spectra.[39,48] The VL was obtained by applying a sample bias of −5 V during the UPS measurements.

The experimental details of MAES are described in Ref. 48. No significant impurity (possibly such as HOGaPc) was observed in x-ray photoelectron spectra for thick ClGaPc films.

III. RESULTS AND DISCUSSION

Figures 2(a) and 2(b) show intensity maps of δ-dependent UPS spectra in the HOMO band and VL regions for the AG and AN films, respectively. A clear δ dependence of the HOMO band onset—the hole-injection barrier (HIB)—is observed for the AG film. The onset of the AG film in Fig. 2(a) shifts continuously to the lower binding energy (E_B) side and finally reaches $E_B = 0.9$ eV, whereas that of the AN film [Fig. 2(b)] stays almost unchanged at $E_B \sim 1.1$ eV. Such an increase in the HIB by annealing was also observed for ClAlPc films/Au polycrystalline electrode in the bottom-contact OFETs, and resulted in a change of the major charge carrier from hole to electron.[23] To elucidate the origin of the difference between δ-dependent ELAs of the AG and AN films, we discuss the details of the electronic structure of these films below.

Figure 3 shows selected UPS spectra in the HOMO band and VL regions of the AG and AN films at $\delta = 0.6$ (AG) and 1.0 (AN) MLE [(near) monolayer], $\delta = 1.9$ (AG) and 2.2 (AN) MLE (near bilayer), and $\delta = 10.3$ (AG) and 8.4 (AN) MLE (thicker films). First, we focus on the AN film below 2 MLE. In Fig. 3, the VL increases continuously up to 1 MLE, and then decreases until 2 MLE. This δ dependence is ascribed to the formation of the well-ordered monolayer (dipole layer) at 1 MLE followed by formation of the bilayer at 2 MLE with a cancellation of P.[35,38,39,41,48] This conclusion is supported by the observation of an asymmetric sharp peak A_1 with a satellite feature (*) due to hole-vibration coupling[10] in the HOMO band at 1 MLE, and appearance of an additional peak A_2 upon the deposition of overlayer molecules. The two peaks A_1 and A_2 could be ascribed to the HOMO of the first and the second layer molecules, respectively, as verified for the OTiPc/graphite system.[36]

In contrast to the AN film, the AG film shows two HOMO peaks from $\delta < 1$ MLE, indicating the formation of bilayer islands from the submonolayer. Peaks A_1 and A_2 still exist in the bilayer spectrum ($\delta = 1.9$ MLE); however, peak A_2 is much broader and peak A_1 is seen as a shoulder due to broadening. Moreover, the VL shift of the AG film, +0.17 eV at 1.9 MLE, is larger than that of the AN film, +0.10 eV at 2.2 MLE. These differences imply that both films are basically regarded as the same structure at the bilayer coverage δ, but the molecules in the AG bilayer film are much less ordered or oriented than in the AN bilayer film,[10] as has been observed also for PbPc/HOPG.[43] This structural difference in the initial film growth is a key for the resulting band bending in thicker AG films, as described below.

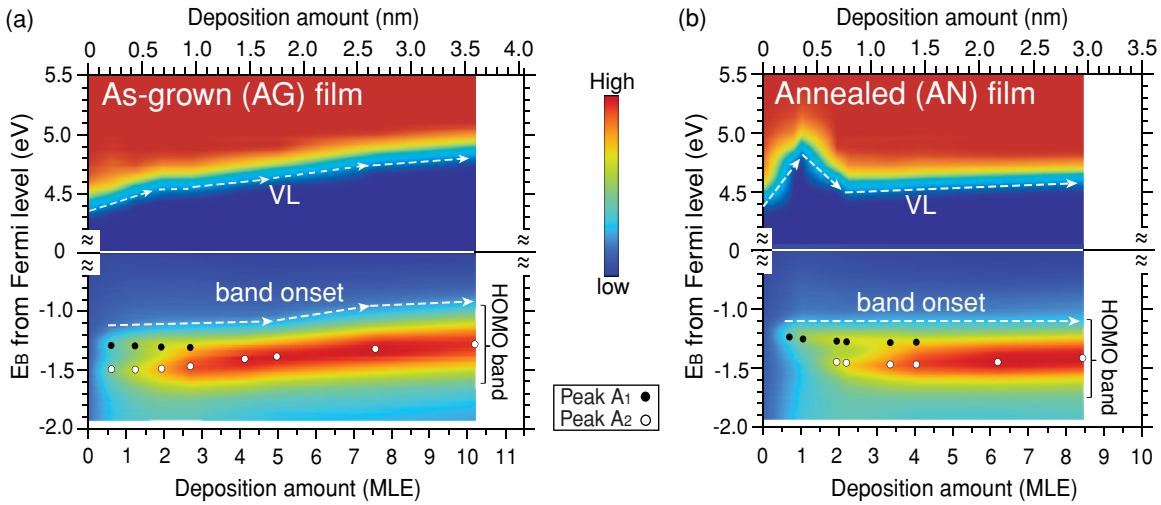

FIG. 2. (Color online) Maps of UPS intensities for the vacuum level (VL) and HOMO band regions of the AG (a) and AN (b) films. The vertical axes represent the binding energy (E_B) relative to the Fermi level, and the horizontal axes represent the deposition amount in nm (top) and MLE (1 MLE = 0.35 nm) (bottom). The black and white filled circles indicate the E_B positions of peaks A_1 and A_2 in the HOMO band [see the spectra in Fig. 3 (left)], respectively. A staircase pattern in the maps originates simply from a larger deposition step.

At larger δs, band A_2 becomes dominant with a single broad band for both the AG and AN film due to the imperfect structure of the films. However, it should be noted again that the HOMO band of the thickest AG film is much broader than that of the AN film and shows a pronounced tailing into the band gap. Such a tailing of the HOMO band [density of gap states (DOGS)] together with the band shift has been observed for organic thin films with structural disorder, and has been considered as a key for control of the ELA of the

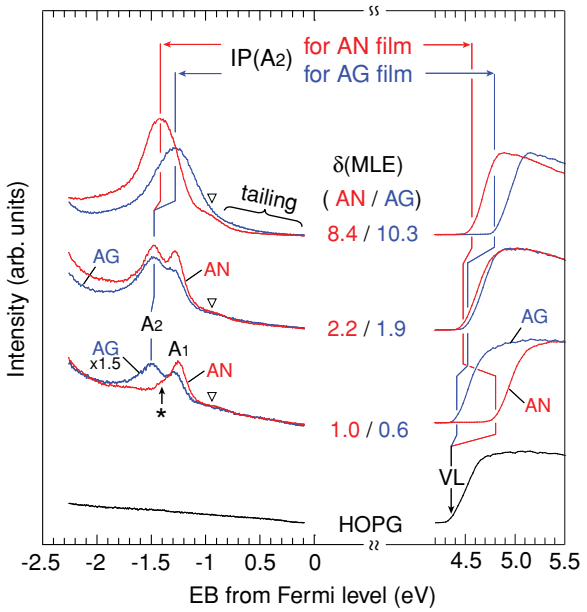

FIG. 3. (Color online) Selected UPS spectra for the VL and HOMO band regions of the AG (0.6, 1.9, and 10.3 MLE; red color) and AN (1.0, 2.2, and 8.4 MLE; blue color) films. * is the vibration satellite in the well-oriented monolayer.[10] The origin of a lower-lying feature (▽) of the main peak seen in the AN films is unclear at the current stage.

systems.[9,12,15,49] Sueyoshi *et al.* demonstrated a strong correlation between the DOGS and ELA for a CuPc/Au system, where the DOGS appear due to disordering of the CuPc molecules by exposing the system to 1-ATM N_2 gas and disappear by annealing.[15] The disappearance of DOGS by annealing was also reported for a pentacene film on a benzenethiolate self-assembled-monolayer/Cu(100) substrate.[50] These results indicate that the HOMO band bending and the VL shift in the AG film are caused by structural imperfections. This model is consistent with the fact that the flat HOMO band and peculiar VL shift were observed after annealing, which induced high order or molecular packing for the AN film, as seen in the energy-level mapping in Fig. 2(b).

To understand the structural imperfections in detail, we compare the ionization potential (IP) of the HOMO band (peak A_2) for the AN and AG films as a function of δ in Fig. 4(a). As the AN film at ~1 MLE consists of the monolayer of downward-oriented molecular dipoles and its structure is largely different from the AG film to show a serious increase in the IP [see Figs. 1(b) and 2(b)],[51] we discuss here the IP for $\delta \geqslant 2$ MLE, where both films mainly consist of a stack of bilayer domains with different structural imperfection. The IPs of the AN film are nearly constant at 6.04 ± 0.02 eV independent of δ for $\delta \geqslant 2$ MLE, whereas the AG film shows a gradual increase for $\delta > 5$ MLE and the IP is 6.11 ± 0.02 eV at $\delta = 10.3$ MLE. To clarify the IP increase, we compare the energy shifts (ΔE) of the VL (ΔVL) and E_B (ΔE_B) positions of peak A_2 above 2 MLE in Figs. 4(b_1) and 4(b_2) for the AG and AN films, respectively. From these comparisons, two important points can be understood for $\delta \geqslant 2$ MLE. First, both ΔVL and ΔE_B are significantly larger for the AG film than for the AN film at any coverage and increase almost identically for $2 \leqslant \delta < 5$ MLE, showing the same IPs for both the films within error bars as shown in Fig. 4(a). Such a behavior that the VL and E_B shifts while retaining a constant IP was also observed for the CuPc/Au system mentioned above by repeating the exposure to 1-ATM N_2 gas and annealing.[15]

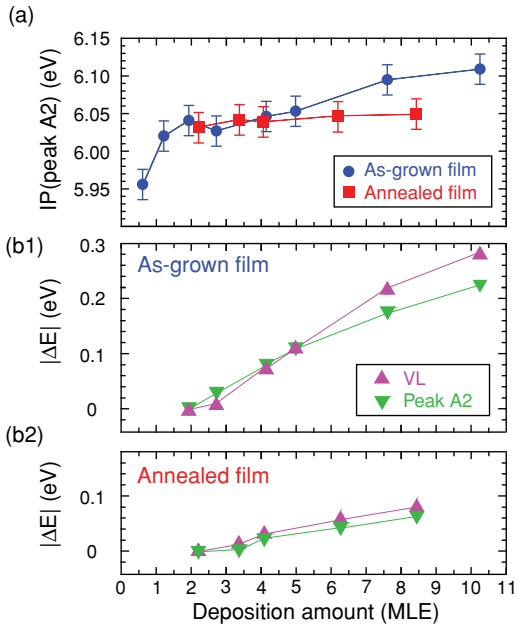

FIG. 4. (Color online) δ-dependent (a) IP (peak A_2) of the AG and AN films and (b_1) a shift in the VL and the position of peak A_2 of the AG (top) and (b_2) AN (bottom) films above 2 MLE. In (b_1) and (b_2), ΔE |represents the VL ($\triangle$) and the E_B of A_2 peak ($\triangledown$) relative to the corresponding values at 2 MLE film.

Therefore, the result is further evidence that the Fermi level moves toward the HOMO band owing to the appearance of DOGS induced by the imperfect ordering or packing of the AG film. Second, ΔVL is clearly larger than ΔE_B of peak A_2 for $\delta > 5$ MLE for the AG film. This explains that the increase in the IP of the AG film for $\delta > 5$ MLE is mainly due to the ΔVL originating from imperfect cancellation of molecular dipoles.

A number of our previous experiments on various p-MPc thin films proved a very similar film growth for OTiPc,[34–37,51] OVPc,[38,51] and ClAlPc[39,51] on graphite and OTiPc[52] and ClAlPc[30–33,52] on MoS_2. In fact, the bilayer domain or island formation and growth are also confirmed from submonolayer thickness for OVPc/HOPG using scanning tunneling microscopy (STM) by Xie *et al.*,[53] which are in excellent agreement with the present results. However, they further found the growth of tilted grains composed of the stacked bilayers at boundaries of the flat bilayer domains or islands in thicker films. In the past, this phenomenon was observed as the δ-dependent inclination of the Pc plane from lying down orientation for ClAlPc/HOPG using high-resolution electron energy loss spectroscopy.[54] Hence the occurrence of the tilted grains seems to be a general tendency for AG films of OMPcs and ClMPcs on HOPG, although their film growth would be largely affected by its condition. To verify such a film growth for the present films, we studied the molecular orientation via δ-dependent MAES spectra. The results are displayed in Figs. 5(a) and 5(b). For reference, the UPS spectrum of the AG film ($\delta = 10.3$ MLE) and the calculated density of state (DOS) of a single molecule obtained by GAUSSIAN 03W package using density functional theory (DFT) [basis set: B3LYP/TVZP] are shown in Fig. 5(c).

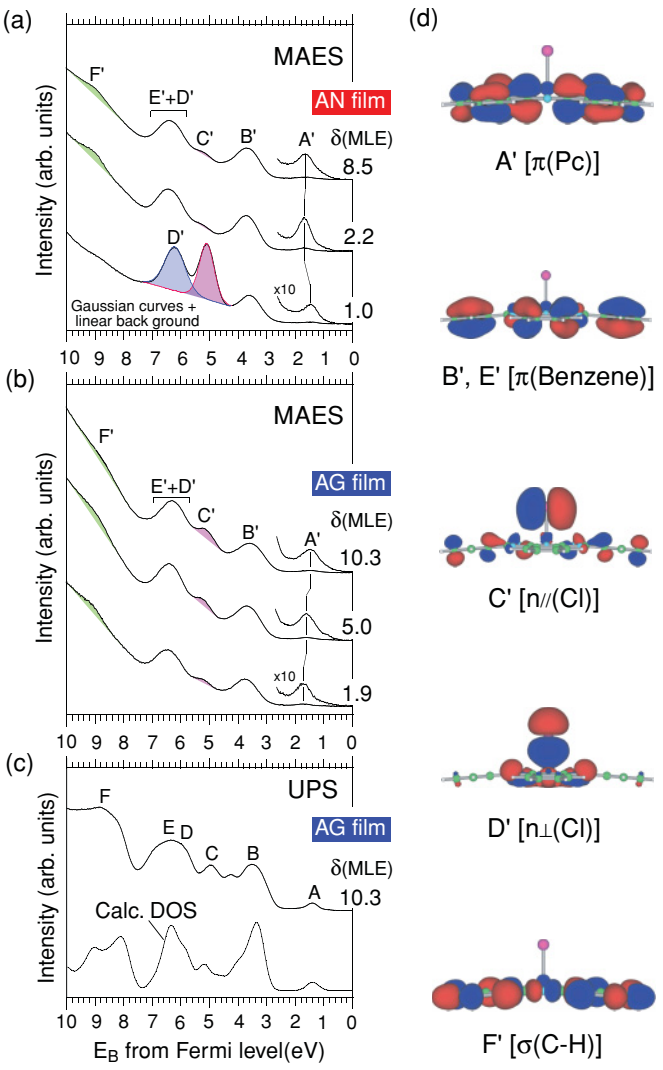

FIG. 5. (Color online) MAES spectra of the AN (a) and AG (b) films at selected thicknesses (δ). (c) The UPS spectrum of AG multilayer film ($\delta = 10.3$ MLE) of ClGaPc/HOPG and the calculated DOS of a single ClGaPc molecule obtained by convoluting calculated molecular orbitals with a Gaussian function (width = 0.5 eV). (d) Schematic of spatial distributions of representative MOs for MAES band A'–F'.

Before discussing Fig. 5, we briefly explain the essence of MAES spectra measured on organic thin films. MAES uses metastable He atoms [(He^*2^3S); 19.82 eV) as a probe, which do not penetrate into the bulk and interact with MOs spreading toward the vacuum side through the Auger deexcitation process (Penning ionization).[55] This process creates one hole in the final state upon ionization so that MAES spectrum shows bands at approximately similar E_B positions as in UPS. Since specific MOs spread more to the vacuum side for certain molecular orientation, e.g., atomic orbitals of the Cl atom for Cl-up orientation of ClGaPc in the present case, and interact effectively with He^*, intense MAES bands illustrate qualitatively but directly the molecular orientation at the outermost surface of the films.[39,48,55]

In Figs. 5(a) and 5(b), a remarkable difference is seen in the AN monolayer ($\delta = 1.0$ MLE) spectrum from other

spectra: The monolayer spectrum in Fig. 5(a) shows very intense bands C' and D', while other spectra show much smaller intensity for those bands and larger intensity for band F'. According to previous studies[31,39,45] and the present UPS and DFT results shown in Fig. 5(c), the bands in the MAES spectra are assigned as follows: band A' is related to a single π orbital of the Pc ring (HOMO band), bands B' and E' to some π orbitals mainly distributed on the benzene rings, bands C' and D' to the nonbonding (n) orbitals of the Cl atom, which are distributed parallel ($\parallel$) and perpendicular ($\perp$) to the molecular plane, respectively, and band F' mainly to σ orbitals distributed parallel to the molecular plane. Spatial distributions of those MOs are shown in Fig. 5(d). As discussed for the UPS results, the AN monolayer film consists of well-ordered Cl-up molecules, while the AN multilayer films and the AG films at all δs are derived from paired Cl-up and Cl-down molecules. Therefore, only the AN monolayer spectrum shows strong bands C' and D' because the He* atoms can interact preferentially with $n_{\parallel}$(Cl) and $n_{\perp}$(Cl) orbitals protruding to the vacuum side for the orientation seen in Figs. 5(a) and 5(b). On the other hand, those bands appear very weakly in all multilayer spectra of both the AG and AN films, where the $n_{\parallel}$(Cl) and $n_{\perp}$(Cl) orbitals are hidden in between the paired molecules and not exposed to the vacuum side. The clear appearance of band F' (σ orbitals) in the AN film above 2 MLE requires tilting of the molecular plane as in the triclinic crystal structure,[44] since π orbitals can shield σ orbitals for the flat-lying Cl-down orientation of the surface molecule. For example, for ClAlPc/MoS_2 systems, the (averaged) tilt angle of the Pc plane was estimated to be 0° (flat-lying) for 1 MLE and ~10° for 5 MLE by angle-resolved UPS.[31] However, importantly, the intensity of band F' does not show any clear δ dependence for the AG and AN films above 2 MLE, which means no drastic change in the tilt angle or no large tilted grains in the present multilayer region for both films.[18,53,54]

On the other hand, the intensity of band C' of the AG film increases with δ in contrast to the AN film. The result evidences an increase of the relative number of Cl-up molecules at the outermost surface of the AG film with δ as expected from Fig. 4(b_1). To demonstrate this point more clearly, we compare the relative intensity of band C' to band $D' + E'$, $I(C')/I(D' + E')$, in Fig. 6(a). This intensity ratio of the AN film for $\delta \leqslant 1$ MLE is much larger than that for any other AG and AN films because all molecules lie flat with the Cl-up orientation for $\delta \leqslant 1$ MLE. For $\delta > 2$ MLE, the ratio of the AG film increases gradually with δ, while this increase is considerably suppressed in the AN film. Moreover, the ratio of the AG film is basically larger than that of the AN film for $\delta > 2$ MLE. The results lead to a conclusion that the AG film has a larger number of the Cl-up molecules for thicker films. This means that the dipoles, due to the Cl-up molecules, are not fully canceled by Cl-down molecules in AG films above 2 MLE, and the number of such Cl-up molecules, which are not paired with the Cl-down molecules, increases in the AG films with δ at the surface of the flat-lying bilayer domains because of no clear observation of the tilted bilayer domains.

In fact, the imperfect cancellation of the molecular dipole was illustrated by STM for ClAlPc/HOPG[40] and SnPc/Ag(111)[56] as either molecular vacancies in the bilayer domains or the occurrence of molecular islands composed of unpaired molecules on molecular layers. However, those structural imperfections could be expected not at all or at least quantitatively much less for the AN film because of the flat-HOMO band and no clear change in the MAES spectra. Accordingly, we expect film structures of the thicker AG and AN films schematically shown in Figs. 6(b) and 6(c),

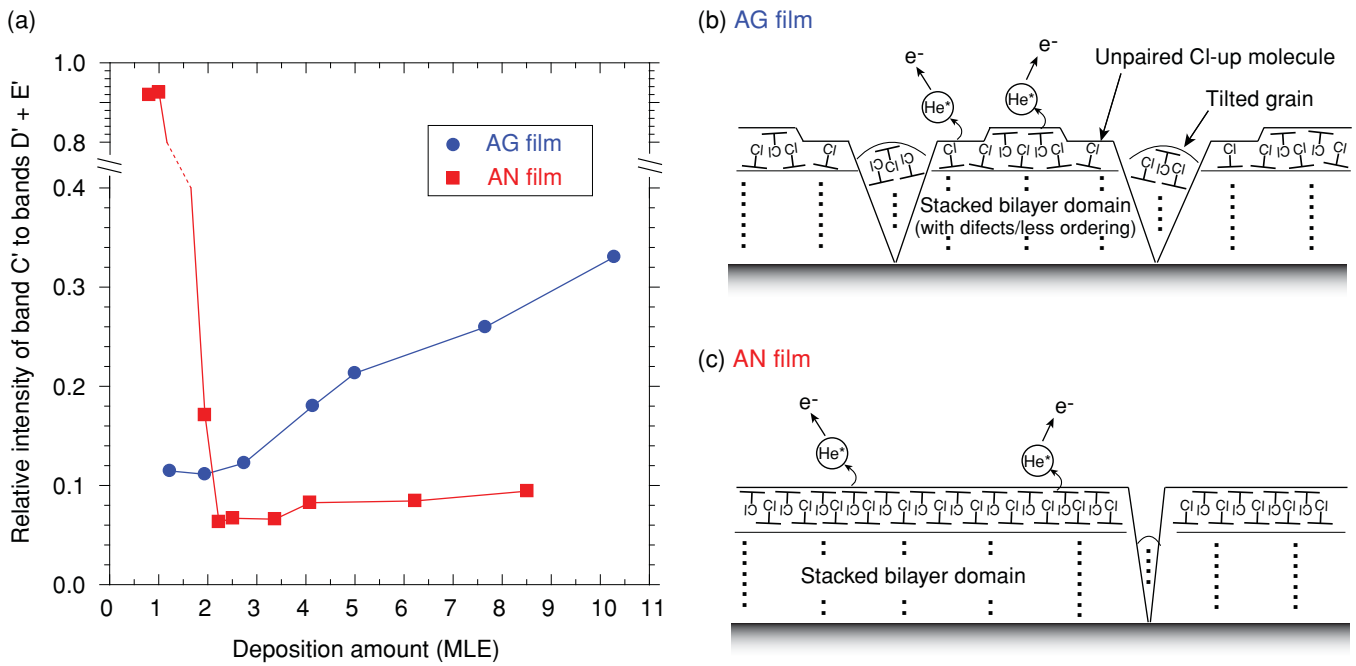

FIG. 6. (Color online) (a) Relative intensity area of band C' to band $D' + E'$ as a function of the deposition amount (δ). The areas are estimated by fitting of those bands with Gaussian curves and linear background [see Fig. 5(a)]. A sketch of the expected structure of the AG (b) and AN (c) films.

respectively. Structural imperfection in the AG film due to the growth of smaller crystal grains or islands with less molecular ordering yields band-gap states by tailing of the HOMO to shift the Fermi level in the gap depending on the density of gap states.[49]

IV. CONCLUSIONS

In conclusion, we revealed how the ELA of polar phthalocyanine films is influenced by their film structure from monolayer to multilayer regions. We observed that the structural defects occur in the as-grown films grown at room temperature and result in a large band bending of the HOMO band toward the Fermi level and a continuous increase in the VL. Furthermore, we demonstrated that these phenomena are considerably suppressed by adopting a simple annealing procedure to yield no serious band bending. The band bending is related to the density of band-gap states originating from HOMO band broadening due to the structural imperfection in the film, which comes from the Fermi level pinning effect throughout the film. We note that such structural imperfections and related gap states also appear in other polar and nonpolar organic semiconductor thin films by external physical perturbation due to, e.g., doping, charge injection, substrate defects and radiation damage, etc.[5,9,12,15,57,58] Therefore, control of the structural imperfections is a key issue for the desired ELA in organic thin-film devices.

ACKNOWLEDGMENTS

The authors thank J. Pflaum for providing the purified ClGaPc and A. Hinderhofer for helpful discussions. T.H. gratefully acknowledges an AvH fellowship for foreign researchers. This work was financially supported partly by the KAKENHI (20685014, 20245039), Global-COE Program of MEXT (G03: Advanced School for Organic Electronics, Chiba University), and the DFG.

*Present address: Department of Materials Science and Engineering, Iwate University, Ueda 4-3-5, Morioka 0208551, Japan; thosokai@iwate-u.ac.jp

†uenon@faculty.chiba-u.jp

[1] H. Ishii, K. Sugiyama, E. Ito, and K. Seki, Adv. Mater. **11**, 605 (1999).

[2] A. Kahn, N. Koch, and W. Gao, J. Polym. Sci., Part B **41**, 2529 (2003).

[3] H. Ishii, N. Hayashi, E. Ito, Y. Washizu, K. Sugi, Y. Kimura, M. Niwano, Y. Ouchi, and K. Seki, Phys. Status Solidi A **201**, 1075 (2004).

[4] M. Fahlman, A. Crispin, X. Crispin, S. K. M. Henze, M. P. de Jong, W. Osikowicz, C. Tengstedt, and W. R. Salaneck, J. Phys. Condens. Matter **19**, 183202 (2007).

[5] H. Fukagawa, S. Kera, T. Kataoka, S. Hosoumi, Y. Watanabe, K. Kudo, and N. Ueno, Adv. Mater. **19**, 665 (2007).

[6] N. Koch, J. Phys. Condens. Matter **20**, 184008 (2008).

[7] N. Ueno and S. Kera, Prog. Surf. Sci. **83**, 490 (2008).

[8] S. Duhm, A. Gerlach, I. Salzmann, B. Bröcker, R. L. Johnson, F. Schreiber, and N. Koch, Org. Electronics **9**, 111 (2008).

[9] J. Hwang, A. Wan, and A. Kahn, Mater. Sci. Eng., R **64**, 1 (2009).

[10] S. Kera, H. Yamane, and N. Ueno, Prog. Surf. Sci. **84**, 135 (2009).

[11] S. Braun, W. R. Salaneck, and M. Fahlman, Adv. Mater. **21**, 1450 (2009).

[12] T. Sueyoshi, H. Fukagawa, M. Ono, S. Kera, and N. Ueno, Appl. Phys. Lett. **95**, 183303 (2009).

[13] Y. Gao, Mater. Sci. Eng., R **68**, 39 (2010).

[14] K. Akaike, K. Kanai, Y. Ouchi, and K. Seki, Adv. Funct. Mater. **20**, 715 (2010).

[15] H. Sueyoshi, H. Kakuta, M. Ono, K. Sakamoto, S. Kera, and N. Ueno, Appl. Phys. Lett. **96**, 093303 (2010).

[16] G. Heimel, I. Salzmann, S. Duhm, and N. Koch, Chem. Mater. **23**, 359 (2011).

[17] D. Beljonne, J. Cornil, L. Muccioli, C. Zannoni, J.-L. Brédas, and F. Castet, Chem. Mater. **23**, 591 (2011).

[18] H. Yamane, Y. Yabuuchi, H. Fukagawa, S. Kera, K. K. Okudaira, and N. Ueno, J. Appl. Phys. **99**, 093706 (2006).

[19] S. Duhm, G. Heimel, I. Salzmann, H. Glowatzki, R. L. Johnson, A. Vollmer, J. P. Rabe, and N. Koch, Nat. Mater. **7**, 326 (2008).

[20] I. Salzmann, S. Duhm, G. Heimel, M. Oehzelt, R. Kniprath, R. L. Johnson, J. P. Rabe, and N. Koch, J. Am. Chem. Soc. **130**, 12870 (2008).

[21] S. Duhm, S. Hosoumi, I. Salzmann, A. Gerlach, M. Oehzelt, B. Wedl, T.-L. Lee, F. Schreiber, N. Koch, N. Ueno, and S. Kera, Phys. Rev. B **81**, 045418 (2010).

[22] S. Kera, Y. Yabuuchi, H. Yamane, H. Setoyama, K. K. Okudaira, A. Kahn, and N. Ueno, Phys. Rev. B **70**, 085304 (2004).

[23] T. Kaji, S. Entani, S. Ikeda, and K. Saiki, Adv. Mater. **20**, 2084 (2008).

[24] C. W. Tang and S. A. VanSlyke, Appl. Phys. Lett. **51**, 913 (1987).

[25] H. Wang, D. Song, J. Yang, B. Yu, Y. Geng, and D. Yan, Appl. Phys. Lett. **90**, 253510 (2007).

[26] L. Li, Q. Tang, H. Li, X. Yang, W. Hu, Y. Song, Z. Shuai, W. Xu, Y. Liu, and D. Zhu, Adv. Mater. **19**, 2613 (2007).

[27] L. Li, Q. Tang, H. Li, and W. Hu, J. Phys. Chem. B **112**, 10405 (2008).

[28] D. Song, F. Zhu, B. Yu, L. Huang, Y. Geng, and D. Yan, Appl. Phys. Lett. **92**, 143303 (2008).

[29] W. Wang, D. Placencia, and N. R. Armstrong, Org. Electronics **12**, 383 (2011).

[30] M. Aoki, S. Masuda, Y. Einaga, K. Kamiya, N. Ueno, and Y. Harada, Mol. Cryst. Liq. Cryst. **267**, 217 (1995).

[31] M. Aoki, S. Masuda, Y. Einaga, K. Kamiya, A. Kitamura, M. Momose, N. Ueno, Y. Harada, T. Miyazaki, S. Hasegawa, H. Inokuchi, and K. Seki, J. Electron Spectrosc. Relat. Phenom. **76**, 259 (1995).

[32] Y. Azuma, M. Tsutsui, S. Kera, M. Aoki, T. Miyamae, K. K. Okudaira, Y. Harada, and N. Ueno, J. Synchrotron Radiat. **5**, 1047 (1998).

[33] Y. Azuma, T. Yokota, S. Kera, M. Aoki, K. K. Okudaira, Y. Harada, and N. Ueno, Thin Solid Films **327–329**, 303 (1998).

[34] S. Kera, K. K. Okudaira, Y. Harada, and N. Ueno, Jpn. J. Appl. Phys. **40**, 783 (2001).

[35]H. Fukagawa, H. Yamane, S. Kera, K. K. Okudaira, and N. Ueno, Phys. Rev. B **73**, 041302(R) (2006).
[36]S. Kera, H. Yamane, H. Fukagawa, T. Hanatani, K. K. Okudaira, K. Seki, and N. Ueno, J. Electron Spectrosc. Relat. Phenom. **156–158**, 135 (2007).
[37]T. Sugiyama, T. Sasaki, S. Kera, N. Ueno, and T. Munakata, Chem. Phys. Lett. **449**, 319 (2007).
[38]H. Fukagawa, H. Yamane, S. Kera, K. K. Okudaira, and N. Ueno, J. Electron Spectrosc. Relat. Phenom. **144–147**, 475 (2005).
[39]S. Kera, H. Yamane, H. Honda, H. Fukagawa, K. K. Okudaira, and N. Ueno, Surf. Sci. **566–568**, 571 (2004).
[40]Y. L. Huang, R. Wang, T. C. Niu, S. Kera, N. Ueno, J. Pflaum, A. T. S. Wee, and W. Chen, Chem. Commun. **46**, 9040 (2010).
[41]S. Kera, H. Fukagawa, T. Kataoka, S. Hosoumi, H. Yamane, and N. Ueno, Phys. Rev. B **75**, 121305(R) (2007).
[42]H. Yasufuku, T. Ibe, M. Okumura, S. Kera, K. K. Okudaira, Y. Harada, and N. Ueno, J. Appl. Phys. **90**, 213 (2001).
[43]I. Yamamoto, N. Matsuura, M. Mikamori, R. Yamamoto, T. Yamada, K. Miyakubo, N. Ueno, and T. Munakata, Surf. Sci. **602**, 2232 (2008).
[44]K. J. Wynne, Inorg. Chem. **23**, 4658 (1984).
[45]T. J. Klofta, T. D. Sims, J. W. Pankow, J. Danziger, K. W. Nebesny, and N. R. Armstrong, J. Phys. Chem. **91**, 5651 (1987).
[46]K. Yamasaki, O. Okada, K. Inami, K. Oka, M. Kotani, and H. Yamada, J. Phys. Chem. B **103**, 13 (1997).
[47]A. Gerlach, T. Hosokai, S. Duhm, S. Kera, O. T. Hofmann, E. Zojer, J. Zegenhagen, and F. Schreiber, Phys. Rev. Lett. **106**, 156102 (2011).
[48]T. Hosokai, M. Horie, T. Aoki, S. Nagamatsu, S. Kera, K. K. Okudaira, and N. Ueno, J. Phys. Chem. C **112**, 4643 (2008).
[49]H. Y. Mao, F. Bussolotti, D.-C. Qi, R. Wang, S. Kera, N. Ueno, A. T. S. Wee, and W. Chen, Org. Electronics **12**, 534 (2011).
[50]A. Kanjilial, M. G. Betti, and C. Mariani, J. Appl. Phys. **104**, 063720 (2008).
[51]H. Fukagawa, S. Hosoumi, H. Yamane, S. Kera, and N. Ueno, Phys. Rev. B **83**, 085304 (2011).
[52]H. Yamane, K. Ito, S. Kera, K. K. Okudaira, and N. Ueno, J. Appl. Phys. **92**, 5203 (2002).
[53]W. Xie, J. Xu, J. An, and K. Xue, J. Phys. Chem. C **114**, 19044 (2010).
[54]Y. Azuma, T. Yokota, S. Kera, M. Aoki, K. K. Okudaira, Y. Harada, and N. Ueno, J. Electron Spectrosc. Relat. Phenom. **88–91**, 881 (1998).
[55]Y. Harada, S. Masuda, and H. Ozaki, Chem. Rev. (Washington, DC) **97**, 1897 (1997).
[56]Y. Wang, J. Kröger, R. Berndt, and W. Hofer, Angew. Chem. Int. Ed. **48**, 1261 (2009).
[57]T. Munakata, T. Sugiyama, T. Masuda, M. Aida, and N. Ueno, Appl. Phys. Lett. **85**, 3584 (2004).
[58]M. Ono, T. Sueyoshi, Y. Zhang, S. Kera, and N. Ueno, Mol. Cryst. Liq. Cryst. **455**, 251 (2006).